Revista Brasileira de Geofísica
RBGf
Brazilian Journal of Geophysics

Revista Brasileira de Geofísica (2017) 35(3): 201-212

ISSN 0102-261X
www.scielo.br/rbg

ACOUSTIC SEISMIC WAVE ATTENUATION IN ROCKS: ESTIMATES INSTABILITIES, FREQUENCY-DEPENDENCE AND INCOHERENCES

Julián Peláez Quiñones and Luis Montes Vides

ABSTRACT. Seismic wave attenuation (Q^{-1}) values indicate relevant media properties, such as fluid content and porosity. Q^{-1} estimates, obtained using both VSP and conventional well log data, did not exhibit comparable trends, nor values. Whereas VSP results represent total attenuation, well log Q^{-1}, which, theoretically, should represent scattering losses, displayed a low percentage correlation with transmission coefficients and other well logs. The influence of processing routines, chosen methodology and input parameters on Q^{-1}-values suggest that ASR (Amplitude Spectral Ratio) and CFS (Centroid Frequency Shift) attenuation estimates should be regarded, in practical terms, as relative quantities instead of absolute ones. Seemingly incoherent negative values are frequent, nonetheless these could hold a physical meaning related to elastic amplification at interfaces. Considering that quality factor (Q) values obtained were more unstable than Q^{-1}-values, it is advisable to report the latter.

Keywords: Vertical Seismic Profiles, well logs, transmission coefficients, scattering, amplification.

RESUMO. Os valores de atenuação da onda sísmica (Q^{-1}) indicam propriedades relevantes dos meios, tais como conteúdo de fluido e porosidade. As estimativas do Q^{-1}, obtidas usando dados de VSP e dados de poços convencionais, não apresentaram tendências nem valores comparáveis. Enquanto os resultados de VSP representam atenuação total, os resultados dos dados de poços, que teoricamente deveriam representar perdas de dispersão, apresentaram uma baixa correlação percentual com os coeficientes de transmissão e outros dados de poços. A influência das rotinas de processamento, da metodologia escolhida e dos parâmetros de entrada nos valores Q^{-1} sugerem que as estimativas de atenuação ASR (Amplitude Spectral Ratio) e CFS (Centroid Frequency Shift) devem ser, em termos práticos, consideradas como quantidades relativas em vez de absolutas. Valores negativos aparentemente incoerentes são frequentes, no entanto estes poderiam conter um significado físico relacionado à amplificação elástica nas interfaces. Considerando que os valores do fator de qualidade (Q) obtidos foram mais instáveis do que os valores de Q^{-1}, é aconselhável documentar o último.

Palavras-chave: Perfis Sísmicos Verticais, registros de poços, coeficientes de transmissão, dispersão, amplificação.

Universidad Nacional de Colombia, Departmento de Geociencias – E-mails: jdpelaezq@unal.edu.co; lamontesv@unal.edu.co

INTRODUCTION

Seismic wave attenuation reduces field data quality and complicates deep data interpretations. On the other hand, quantifying attenuation supports rock (and its fluid content) characterization; indicating permeability, liquid/gas presence and saturation. Although Vertical Seismic Profiling (VSP) data is usually employed to estimate attenuation, authors have proposed to employ conventional well logs for such task, since these are usually cheaper and easier to acquire. Nonetheless, debate persists regarding the validity of velocity-based attenuation estimates, as opposed to the waveform methodology. Even if full-waveform Sonic logs are used to measure attenuation, it is generally accepted that high-frequency waves do not obey the same absorption phenomena as those of seismic frequencies. Liner (2014) proposes to apply Backus averaging of conventional Sonic log along with Density log to obtain seismic-frequency scattering attenuation.

We study the meaning of attenuation results obtained by velocity dispersion analysis of conventional Sonic log using Liner's (2014) method. These are compared to VSP attenuation results (using Amplitude Spectral Ratio and Centroid Frequency Shift methodologies), transmission coefficients, and other well logs. Additionally, we depict the influence of input parameters and processing routines on attenuation estimates, and their eventual limitations and apparent incoherences are analyzed, such as the instability of quality factor values; the use of attenuation as a relative quantity instead of an absolute rock property in practical applications; and the recurrence of negative attenuation values, which might hold a physical meaning.

THEORETICAL BACKGROUND

Besides geometrical spreading, experimental issues and noise, only absorption should be responsible for amplitude variations of waves in homogeneous media. Nevertheless, wave mode conversion and elastic effects attenuate wave pulses in heterogeneous media only apparently, since their total energy is conserved though spatially redistributed. The degree of absorption is expressed through the Quality factor (Q), defined in Aki & Richards, 2002 (pgs. 162–171). Whereas Q is, by definition, related to viscoelasticity alone, in practice it is a superposition of all mechanisms that alter wave amplitude, including scattering. Therefore, ignoring experimental issues; interference; and geometrical spreading, attenuation (Q^{-1}) is often broken down into the following linear superposition (Alasbali et al., 2016):

$$Q^{-1}_{total} = Q^{-1}_{intrinsic} + Q^{-1}_{scattering}, \qquad (1)$$

where Q^{-1}_{total} represents effective attenuation. The Scattering term ($Q^{-1}_{scattering}$) represents elastic attenuation related to acoustic impedance contrasts between adjacent media. If constant Q theory (Kjartansson, 1979) is assumed within the appropriate frequency range, Q^{-1} becomes frequency-independent, although this is only valid within seismic frequencies (whose exact limits are medium-dependent). High intrinsic attenuation is related to fluid content, low permeability and vuggy porosity (Parra et al., 2015).

METHODS

Q^{-1}_{VSP} estimation

VSP and well logs dataset in this study belong to colombian Llanos Orientales sedimentary succession, comprising interbedded sandstones and mudstones with minor variations of grain size and vertical thickness. VSP data comprises the Y component of a zero-offset VSP survey. In total, 57 Traces were available. Shallowest trace is 305 m-deep and deepest one is at 983 m. Total record time equals 3,6 seconds, and $f_{sampling}$ =1000 Hz. The processing consisted of static corrections and application of 5-trace-wide alpha-trimmed spatial 2D filter to separate downgoing and upgoing wavefields. Deterministic deconvolution and a Ormsby band-pass filtering were both applied equally for all traces within 10 and 100 Hz in order to suppress multiples, instrumental effects and noise. These processes do not corrupt ASR results and CFS trends are only weakly affected, while on the other hand they considerably improve the accuracy of the first-break picks, fundamental for the reliability of both methods.

Cumulative values ($Q^{-1}_{cumulative}$) are obtained by using a fixed reference trace, whereas interval values ($Q^{-1}_{interval}$) are obtained by comparison of successive traces. Attenuation is assumed nearly constant within seismic domain, so that VSP analyses are carried out at depth, not in frequency. Various reference traces were tested for $Q^{-1}_{cumulative}$ estimates. Frequency ranges (bandwidth) for ASR regression remained between 10 and 90 Hz. A Daniell window for amplitude spectra smoothing was useful to avoid noisy peaks.

Time windows for smoothing with various sizes were applied to check their influence on $Q^{-1}_{interval}$ and $Q^{-1}_{cumulative}$ results. The first VSP method employed is Amplitude Spectral Ratio method (ASR – Rutledge & Winkler, 1989), whose fundamental equation is:

$$\ln\left(\frac{A_1(f)}{A_0(f)}\right) = \ln G - Bf, \qquad (2)$$

A represents amplitude spectrum of an arrival, B equals

$\pi(x_1 - x_0)/vQ_{ASR} = \pi(t_1 - t_0)/Q_{ASR}$, where v is effective velocity and t is the first-break pick time. One notices that this relationship expresses a straight-line equation, being G the vertical intercept and $-B$ the slope in a frequency (f) against $\ln(A_1(f)/A_0(f))$ plot. Having the arrival time (t_1) up to certain depth x_1 and using another trace as reference (x_0, t_0), it is possible to determine Q^{-1}_{ASR}. The second VSP method here employed is Centroid Frequency Shift (CFS – Quan & Harris, 1997), whose fundamental idea is to compare the centroid frequencies of the direct wave spectra (assumed Gaussian) at increasing depths, which should decrease since the high-frequency components are eliminated as the wave propagates. The CFS main equation is:

$$Q_{CFS} = \frac{\pi\sigma_0^2\Delta t}{f_{c0} - f_{c1}}, \tag{3}$$

where Δt is the travel time difference between arrivals of a given and a reference trace with centroid frequencies f_{c01} and f_{c0}, respectively. σ_0^2 is the variance of the reference arrival. Both methods were chosen in view that these are usually employed to estimate attenuation from VSP data, plus, probably the ones that yield highest quality-to-procedural complexity ratio.

Q^{-1}_{log} estimation

Well logs (Caliper; SP; Gamma Ray; Resistivity; Density; Neutron Porosity and Sonic P-wave), allowed correlation with attenuation logs, as well as lithology interpretation. Well log sampling interval (dz) is 0.5 ft ($\approx$ 15 cm). Data is quality-checked and corrected for borehole width, temperature, pressure and mud weight. Sonic log was available from depths 878 to 990 m (2880 to 3250 ft).

Log attenuation estimation method

Liner (2014) methodology relies on Backus long-wave theory (Backus, 1962) and Kjartansson's constant-Q theory (Kjartansson, 1979). Liner specifies that this method yields scattering attenuation alone. VSP methods account for total attenuation.

The procedure consists of approximating normal-incidence seismic P-wave velocity ($v_{p0}^{seismic}$) from Sonic P-wave velocity (v_p^{sonic}) by using the linearized velocity formulation of a vertically-traveling wave in a medium with vertical symmetry axis ($<>$ denotes average):

$$v_{p0}^{seismic} = \sqrt{\frac{C_{33}}{<\rho>}} = \left[\frac{1}{<\rho>}\left\langle\frac{1}{\rho(v_p^{sonic})^2}\right\rangle^{-1}\right]^{1/2} \tag{4}$$

via the relationship $C_{33} =< c_{33}^{-1} >^{-1}$ (Backus, 1962), where $c_{33} = \rho(v_p^{sonic})^2$, ρ is density and C_{33} is one of the seismic elastic moduli of the stiffness tensor for orthorhombic or higher symmetry rock layer, isotropic and with principal axes consistently oriented (Tiwary et al., 2009).

After randomly defining L_B, constrained by the relationship $H_{layer} < L_B < \lambda_{\min}$ (H_{layer} is mean layer thickness and $\lambda_{\min}$ is minimum seismic wavelength), applying Kjartansson's dispersion relationship (Kjartansson, 1979) yields:

$$Q^{-1}_{log} = \tan\left[\frac{\pi\ln(v_{p0}^{seismic}/v_0)}{\ln(v_{p0}^{seismic}/v_0) + \ln(\lambda_0/\lambda)}\right] \tag{5}$$

λ_0 and v_0 are reference wavelength and reference velocity, respectively. Liner (2014) proposes to use $\lambda_0 = L_B$, $\lambda = dz$, and v_0 as the sonic velocity; nevertheless, if coherence between domains is to be kept, wavelength values should be exchanged: $\lambda_0 = dz$ and $\lambda = L_B$ (or velocities could be switched instead); in this study, $\lambda_0 \approx 0.15$ m and $\lambda \approx 9.1$ m.

RESULTS

Q^{-1}_{VSP}

ASR method

Different smoothing functions yield the trends shown in Figure 1. Due to the low attenuation values obtained, slight Q^{-1} variations mean significant Q variations and peaks (Fig. 1a). Negative Q values are progressively higher for Hamming, Hann and Blackman windows, with abundant $|Q| >$100 (the typical maximum value for rocks), while flat-top window generated the highest positive values in overall, except for a peak with inverted polarity (with respect to the former windows) around 2200 ft (Fig. 1a). This evidences the fact that Q peaks and negative values can also result from windowing.

Whereas Q^{-1} (Fig. 1b) emphasizes strata which attenuate (or, apparently, amplify) seismic waves considerably, Q peaks (regardless of their polarity) only point out intervals which preserve wave amplitude. Moreover, according to Density-Neutron crossplot (not shown), most negative Q^{-1} peaks coincide with gas-saturated intervals, while Q peaks presented no clear correlation with lithology anomalies.

Bandwidths below 70 Hz yielded a smaller amount of negative values than those reaching 90 Hz (Fig. 2a). The lowest bandwidth (10-70 Hz) had the highest values, while the bandwidth in-between (30-60 Hz) behaved more or less as their average. Shifting and scaling of trends is observed. $Q^{-1}_{interval}$ was also sensitive to bandwidth chosen: numerical values of peaks differ considerably, and inversions for different bandwidths is present (see peak just above 3000 ft in Fig. 3a). Here, 10-70 Hz bandwidth exaggerates interval attenuation values, in overall, the least.

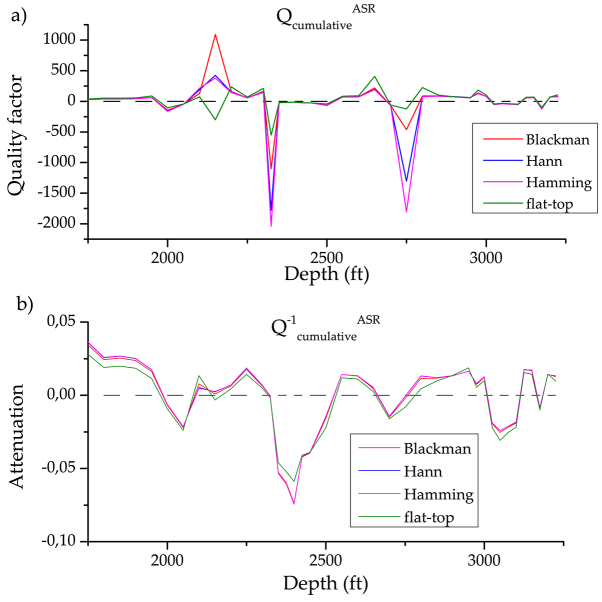

Figure 1 – Influence of time windowing on Q and Q^{-1} estimations: a) $Q_{cumulative}$ estimated through ASR method using the 5th trace as reference (out of the 57 traces) and bandwidth 15 to 90 Hz; b) Q^{-1} for the same interval.

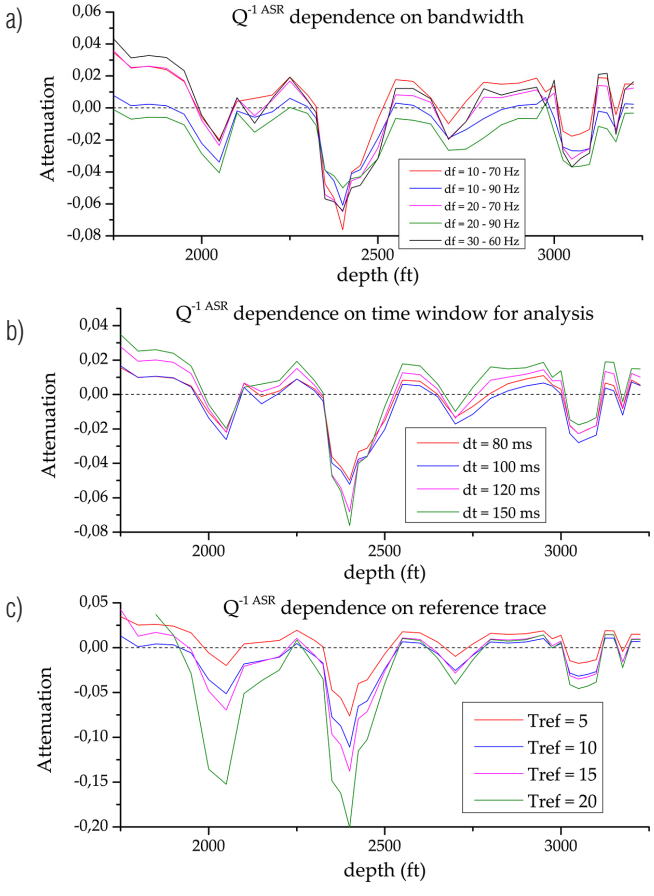

Figure 2 – Parameter influence on ASR $Q_{cumulative}^{-1}$ estimations (fixed parameters in parentheses): a) bandwidth (frequency range for regression – dt=150 ms; Tref=5); b) time window (Tref=5; df=10-70 Hz); and c) reference trace (dt=150 ms; df=10-70 Hz).

Time window chosen was the parameter least prone to generate instabilities in both, cumulative and interval values, although widening the time window slightly upscales the attenuation response while the trend remains unaltered (Figs. 2b and 3b). Reference trace chosen affected $Q^{-1}_{cumulative}$ values (more than bandwidth choice did) by exaggerating peaks and shifting the plots "downward" as reference trace was deeper (Fig. 2c).

$Q^{-1}_{interval}$ presents numerous peaks more than a magnitude order higher than those of $Q^{-1}_{cumulative}$ (Figs. 2 and 3), specially in the deepest part of the section, although a careful comparison of both graphs indicates comparable trends. $Q^{-1}_{cumulative}$ represent the cumulative effect of each layer and interface on the traveling pulse, thus their values should be higher than those of $Q^{-1}_{interval}$. This anomalous result can be explained in terms of ASR regression slope: if the travel time difference between traces is low, as it is between neighbor receivers, attenuation is overestimated. Moreover, the use of deeper traces as comparison reference yields unreliable values, receiver sensitiveness and noise play an increasingly important role on the subsequently smaller amplitudes measured at depth. Nevertheless, it is remarkable that $Q_{cumulative}$ exceeded the expected range of values for rocks ($10 \sim 200$), while $Q_{interval}$ values remained below this range.

CFS method

Similar parameters to those of ASR were tested for CFS method. Relatively small Q^{-1} fluctuations appear when using different time windows (Fig. 4a); the values generated by the shortest (80 ms) and the largest (150 ms) windows tend to enclose those of the windows in-between. Reference trace, again, yielded the highest instability on the results, as it is depicted in Figure 4b. Shallowest reference traces returned few peaks and acceptable values, while using the rest of them generated unstable and exaggerated values. It is thus recommended to employ shallower reference traces for $Q^{-1}_{cumulative}$ estimations, although this implies a trial-and-error procedure, considering that shallowest traces are sometimes saturated or noisy.

Centroid frequencies calculated over the entire time range yielded a coherent decreasing trend at depth in some sections, yet, source decoupling and aliasing might result on the opposite trend. In order to obtain decreasing frequencies, it was necessary to restrict the spectral window for calculations to a range between 0-35 Hz, otherwise, depth-increasing centroid frequencies were common.

Figures 2 and 4 depict the similarity between ASR and CFS Q^{-1} trends and values.

Q^{-1}_{log}

Q^{-1}_{log} analysis is carried out within the Sonic log interval. The influence of weighting function on Sonic velocity is shown in Figure 5. Using rectangular or Gaussian function is almost indistinguishable, nonetheless, Blackman and Hanning functions do conserve relative peaks polarity, while the former invert them as a function of window size owing to the relationship between sonic log spatial frequency variations and window size (the wider the window, the more probable are peak inversions). Blackman and Hanning functions do not fulfill all weighting average conditions stated in Backus (1962); however, their results do not alter the raw data trend. Dependence of Density log on weighting function and window size is the same as for sonic velocity.

The influence of averaging type for our dataset is show in Figure 6; it does not appear necessary to apply Backus-type average of velocities, since these do not differ considerably from the arithmetic average results. A direct implication is that Density log may not be necessary as a parameter for this method, unless very large or very small density outliers are present, in which case, harmonic and arithmetic averages of density will differ considerably in Eq. (4).

L_B choice has few constraints, other than the requirement of being comparable to common seismic wavelengths, which are in the range $10 \sim 300$ m. Moreover, L_B also depends on the distance covered by field data, in our case, it comprised ≈110 m, thus if averaging windows as wide as 60 m are applied, less than half of the interval would allow Q^{-1}_{log} estimations.

Figure 7a illustrates the attenuation results (in green), along with VSP and Sonic transmission coefficients (T_0^{VSP},T_0^{sonic}). Attenuation includes negative and near-zero values (infinite quality factor). The antisymmetric (around zero-offset) normalized cross-correlation between Log attenuation and T_0^{sonic} (Fig. 7b) indicates that, although their trends are comparable, the two signals are ≈2 ft shifted (also evident in Fig. 7a). The ambiguity at zero-offset can be related to averaging window width used previously to determine $v_{p0}^{seismic}$, resulting in shifted attenuation estimates. A maximum negative match of nearly -20% occurs at zero offset. It is assumed that the correct fit should be the negative one instead of the positive, since the latter would imply that amplification corresponded to transmission coefficients < 1.

Fit between Log attenuation and T_0^{VSP} is maximum ($\approx -20\%$) at zero-offset, even though they present a sampling mismatch and, consequently, depth of sharp interfaces have uncertainties of about 25 ft (mean receiver separation). T_0^{VSP} were obtained from a VSP velocity model. Although these percentages of maximum correlation are somewhat low, they are negative,

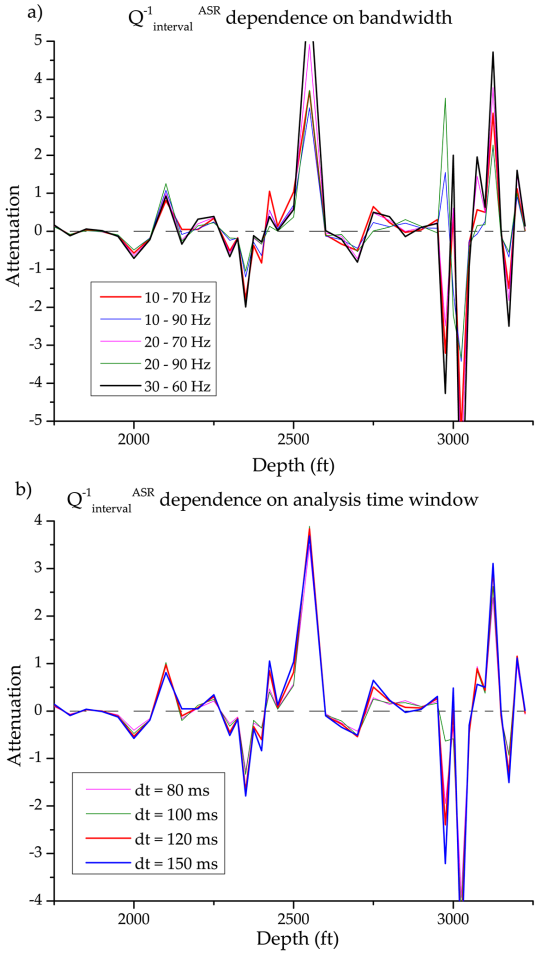

Figure 3 – Parameter-dependency of $Q^{-1}_{interval}$, estimated through ASR method, on: a) bandwidth (df=10-70 Hz), and b) time window for analysis (dt=150 ms).

partially agreeing with the fact that Q^{-1} might represent scattering attenuation. Nonetheless, high and low frequency impedances are generally not equivalent, so that Q^{-1}_{log} response could depict Sonic-frequency regime, but not necessarily that of seismic frequency.

DISCUSSION

Negative attenuation

Negative Q^{-1} values were found for all of the methods employed. It is considered as non-physical for $Q^{-1}_{intrinsic}$ to take these values, since absorption does not amplify waves; nevertheless, it appears inherent to the methodologies employed, along with source/ receiver decoupling, interference and noise, to generate these negative values, which are often reported (Suzuki & Matsushima, 2013; Bouchaala et al., 2016). Even so, wave amplification could correspond to a phenomenon unrelated to energy creation during propagation, if we consider that Q^{-1} estimation through these methods yields a combined response of intrinsic and scattering effects. Since only elastic effects should generate $Q^{-1}_{scattering}$, the normal-incidence oscillation velocity transmission coefficient (Fox Smith, 2010) is, thus, a proxy for scattering losses:

$$T_{12} = \frac{A_T}{A_0} = \frac{2Z_1}{Z_1 + Z_2} \tag{6}$$

where $Z_i = v_i\rho_i$ and A_T, A_0 are transmitted and incident amplitudes, respectively. Eq. (6) applies for normally-inciding waves traveling from medium 1 into medium 2, although normal-incidence is approximate for zero-offset VSP ray-paths. By taking $Z_2 \to 0$ in Eq. (6), it follows that $T_{12} \to 2$, leading to the inequality $0 < T_{12} < 2$ (King, 2009). Under these conditions, $T_{12} > 1$ implies $Z_1 > Z_2$ and that local amplification is possible; yet, does this imply a violation of the conservation of energy

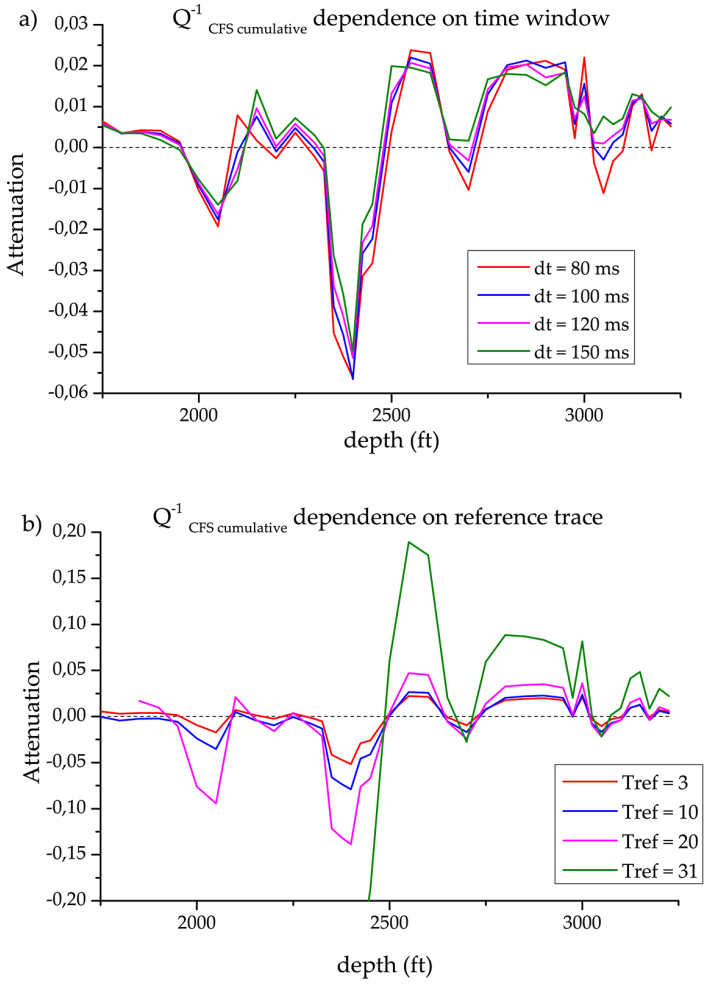

Figure 4 – $Q^{-1}_{cumulative}$ estimated through CFS method and its dependence on: a) time window (dt=80 ms), and b) reference trace (Tref=4).

principle? Let us consider the total instantaneous energy density of an isotropic elastic medium during the propagation of a plane wave, given by (Sheriff & Geldart, 1995):

$$W = \frac{1}{2}\rho A^2 \omega^2 \tag{7}$$

If $Z_1 \neq Z_2$, it is necessary that the energy density of the incident wave is higher than that of the transmitted wave ($W_0 > W_T$); thus for any frequency ω:

$$\frac{1}{2}\rho_1 A_0^2 \omega^2 > \frac{1}{2}\rho_2 A_T^2 \omega^2 \tag{8}$$

Accordingly, the normal-incidence energy transmission coefficient (E_{12}^T) satisfy (Pain, 2005)

$$0 < E_{12}^T = \frac{4Z_1 Z_2}{(Z_1 + Z_2)^2} = \frac{Z_2}{Z_1} T_0^2 < 1, \tag{9}$$

along with the condition $E_{12}^T + E_{12}^R = 1$ (E_{12}^R is normal-incidence energy reflection coefficient), which confirms that Eq. (6) does not lead to energy creation, since Eq. (9) is an implication of the former. Wave pulses that amplify at interfaces simultaneously reduce their intensity. Using Eq. (6), a substitution of A_T in Eq. (8) yields:

$$\rho_1 > \rho_2 T_{12}^2, \tag{10}$$

which, in turn, combined with Eq. (9) yields:

$$v_2 > v_1 E_{12}^T, \tag{11}$$

meaning that when medium 1 has a higher density, specifically greater than T_{12}^2 times that of medium 2, or equivalently, if 2-to-1 media velocity ratio is higher than the fraction of energy transmitted, amplification could occur; keeping in mind that geological

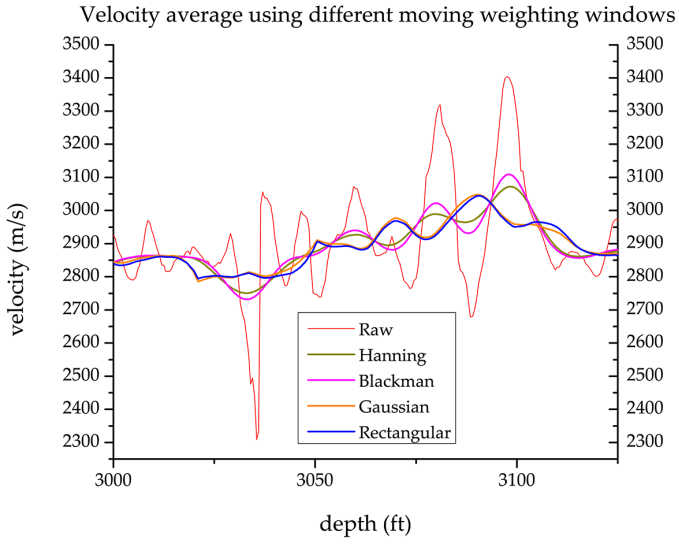

Figure 5 – Sonic log raw data (red) and Backus-averaged velocities in a segment of the interval of interest after different weighting functions. Averaging window width is $\approx 9,1$ m ≈ 30 ft.

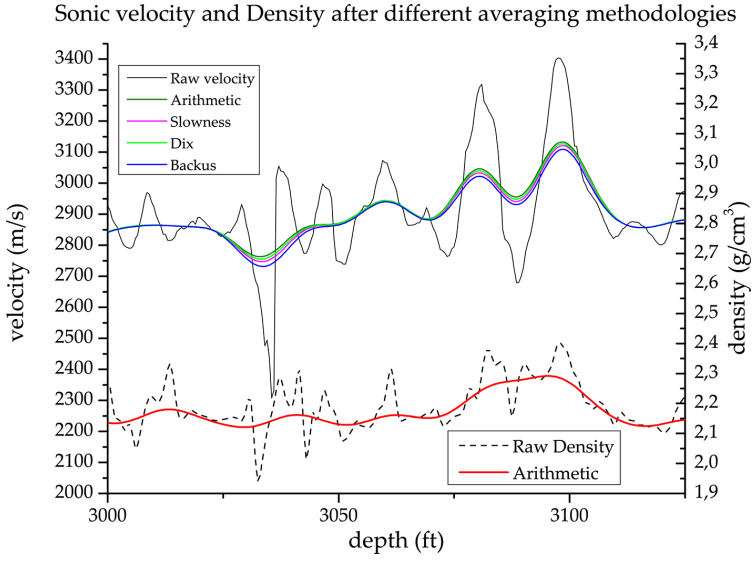

Figure 6 – Averaged Sonic velocity and Density log; the influence of average methodology on the former is depicted. 60-samples Blackman window was applied.

media are not completely elastic and that geometrical spreading also affects wave amplitude, preventing indefinite amplification.

Alternatively, the amplification condition can also be expressed in terms of density and elastic moduli (M), considering $v_i = \sqrt{M_i/\rho_i}$. For normal-incidence oscillation velocity coefficients, condition $Z_1 > Z_2$ becomes:

$$\frac{\rho_1}{\rho_2} > \frac{M_2}{M_1}, \tag{12}$$

while such condition for normal-incidence pressure amplitude, whose transmission coefficient is $2Z_2/(Z_1 + Z_2)$, would be:

$$\frac{\rho_1}{\rho_2} < \frac{M_2}{M_1} \tag{13}$$

Moreover, Liner (2014) shows that his negative Q^{-1} results do not lead to a divergent wavefield, and relates them to local amplification due to elastic phenomena. Gas-saturated rock intervals have lower densities and impedances than the same compacted rocks, such that negative Q^{-1} values could suggest these marked acoustic impedance contrasts.

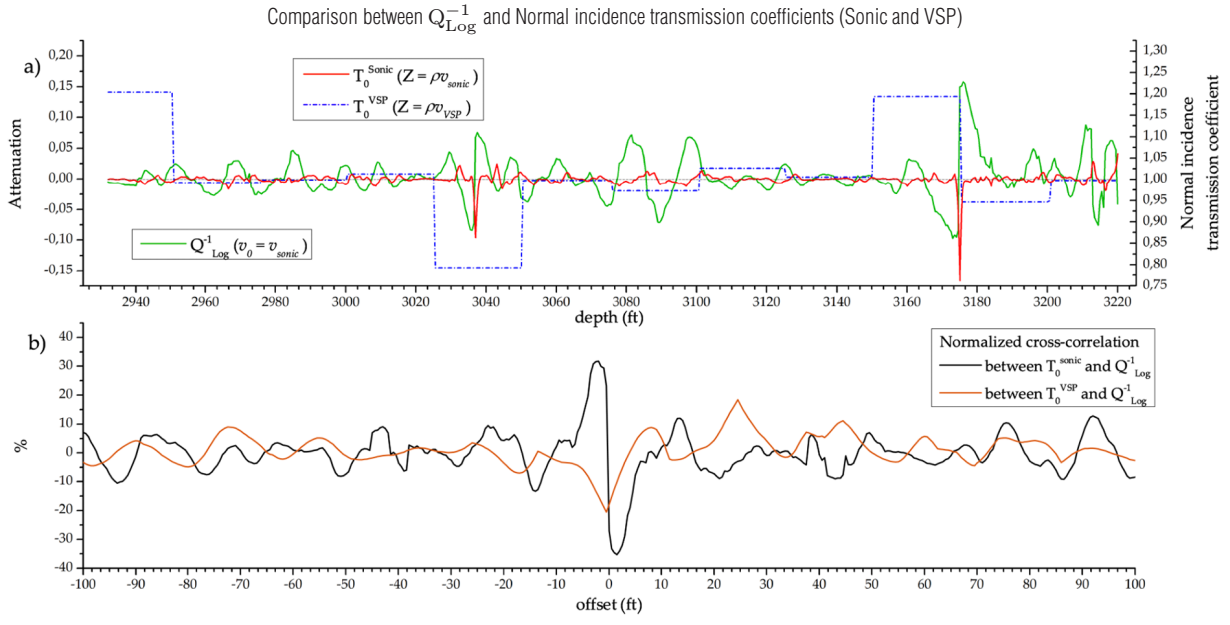

Figure 7 – a) comparison between Liner attenuation estimates and normal-incidence transmission coefficients (from Sonic log and VSP). b) normalized cross-correlation between L-B-K attenuation and normal-incidence transmission coefficients.

Attenuation logs and comparisons

Figure 8 depicts attenuation estimates obtained using the different methods here applied. The degree of similarity between ASR and CFS interval attenuation results can be appreciated, as well as the low similarity between Log and VSP results. This might point out that:

1) because Q^{-1} is constant only within a low frequency range and seismic and log domains presents different wavelength-heterogeneity size relationships and, accordingly, different attenuation phenomena, their results should not be taken as equivalent; or

2) the interpretation for each case is different, e.g. while VSP results indicate total attenuation, those of Log method could provide, at least partly, scattering attenuation.

For comparison, relative shale volume along the interval of interest is included in Figure 8. Clavier et al. estimation (Bassiouni, 1994), using Gamma Ray log, is employed. High shale volumes are clearly related to high porosity, but only partially to VSP attenuation. Figure 8 also depicts the sampling mismatch between VSP attenuation and well logs. Around 2990 ft there is a background variation from high to low shale volume which coincides with a high VSP attenuation interval, as expected. A sandy above a shaly interface (low to high porosity) around 3020 ft matches a VSP amplification but, still, clear correlation is not always possible. On the other hand, a couple negative Log attenuation peaks coincide with shale volume and porosity anomalies (3035, 3090 and 3170 ft), while steady intervals are comparable (above 3000 ft and between 3100 and 3160 ft). Nevertheless, it is unclear from Liner's method attenuation log whether attenuation or amplifications occurs at each of the depths mentioned.

Resistivity log is sensitive to fluid content, and although it does not have a good correlation with Q^{-1}_{log} in Figure 8, its 3020 ft-peak coincide with $Q^{-1}_{VSP} < 0$ (ASR and CFS); this could be interpreted as local intrinsic amplification owing to fluid content; yet the 3000 ft Resistivity peak, on the contrary, coincides with a high attenuation, introducing ambiguity into interpretations. Moreover, some Q^{-1}_{VSP} anomalies (e.g. 2970 ft) are not reproduced in any well log. The deepest interval (3170 ft) has an underlying high impedance and low porosity formation that coincides with a VSP amplification, while Log attenuation depicts a mixed trend: an amplification related to a high porosity (high shale volume) followed by a decay until 3180 ft, where porosity drops. This behavior of Q^{-1}_{log} is consistent with the transmission coefficients and their amplification condition.

If Liner method is to be used for Q^{-1} estimation, it is debatable whether it brings additional information that the transmission coefficients, or the Sonic log itself (whose inverse trend is almost identical to that of Q^{-1}_{log} in Fig. 8), do not. Regarding λ, it is rea-

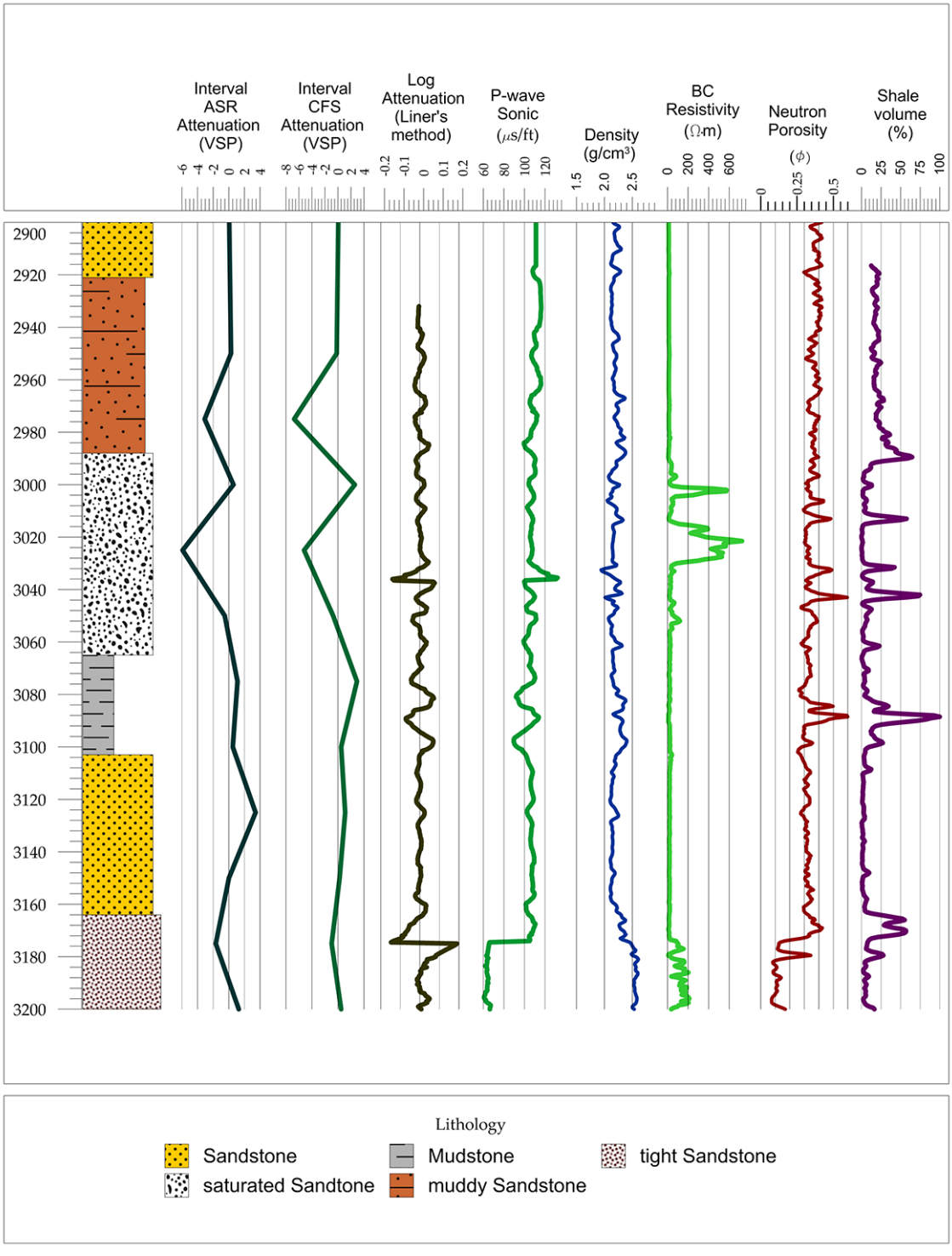

Figure 8 – Different attenuation results obtained, together with different well logs for comparison. General lithology column interpreted from well logs altogether. The deepest sandstone differs from the overlying on account of its higher cementation and density, and low porosity. Depth in feets.

sonable to think that since v varies, so should λ, yet, Liner (2014) chooses λ as constant for every velocity. This simplification appears necessary in order to apply Eq. (5), but poses a limitation of the method itself, along with the assumption of a VTI layered Earth.

Final remarks

ASR method is very sensitive to bandwidth, e.g. when using a range 15∼100 Hz, Q_{ASR}^{-1} had an exactly opposite (negative) trend compared to that of Q_{CFS}^{-1}; when it was reduced to 20∼70 Hz, both plots had same signs at each depth. This shows the sensitiveness of some datasets to linear regression of amplitude ratio. In overall, CFS method is simpler than ASR, but both yielded very similar trends for our data, being the largest difference their numerical values, which may not be a determinant signature, unlike their relative trends.

These methods are useful for practical applications, such as correlations, but the values they yield may be meaningless or unreliable if a determinant property related to a specific lithology, fluid content or another rock signature, is intended. Bearing this in mind, it can be appropriate to report attenuation as a normalized quantity at depth for a given survey.

It is advisable to try out different windows, yet, weighted windows (such as Blackman) are preferable over rectangular for smoothing. In our case, time windows from 100 to 150 ms and bandwidths from 20 to 70 Hz performed well (frequencies above ≈90 Hz should be avoided). For CFS method, static deconvolution suppresses multiples while distorting the raw spectra, so it is advisable to compare results with and without these procedures to detect intervals with lesser degree of confidence; in our case, variations were only locally substantial in comparison to ASR results, which in turn has the advantage of remaining unaffected by such routine. Special care should be taken when first-break picking to avoid further instabilities.

Assuming that $Q_{log}^{-1} = Q_{scattering}^{-1}$, the significant difference between Q_{VSP}^{-1} and Q_{log}^{-1} values challenges Eq. (1); is this linear superposition generally valid? If so, scattering attenuation would be negligible and intrinsic attenuation could be found directly from VSP, at least in our case.

CONCLUSIONS

Q-values presented a numerical variation higher than that of Q^{-1}-values in response to input parameters. Q peaks indicate only rock successions that do not attenuate (nor amplify) seismic waves considerably, while Q^{-1} peaks do depict them. Moreover, attenuation values express a more straight-forward physical meaning. ASR and CFS methods appear useful to find relative Q^{-1} values, rather than absolute attenuation; this fact should be considered, in particular, by the interpreter of seismic data.

Liner's (Log) and VSP attenuation estimates differ considerably, indicating that their results did not correspond to the same rock property. Log attenuation correlates partially with sonic transmission coefficients and other well logs, thus it could be used as an (approximate) proxy for scattering attenuation. Nevertheless, its trend mimics that of Sonic log, which would be sufficient for analyses. Moreover, transmission coefficients represent normal-incidence scattering more clearly.

Negative Q^{-1} values, although apparently incoherent, could correspond to the added effect of error sources and the scattering process itself, which can locally amplify oscillation (particle) velocity of downward-traveling wave pulses at interfaces if the acoustic impedance of the underlying medium is lower than that of the overlying medium, while conserving its transmitted elastic energy.

ACKNOWLEDGEMENTS

Thanks to Deco's RadExPro Professional 2016 software developers and company for providing a demo version of their software for VSP processing, as well as to all developers of software employed for data management. The authors also thank two anonymous reviewers for comments and suggestions and to all the authors and sources of knowledge that allowed outcome this work.

REFERENCES

AKI K & RICHARDS P. 2002. Quantitative Seismology. 2nd ed., University Science Books, Sausalito, California. 948 pp.

ALASBALI A, PEVZNER R, TERTYSHNIKOV K, BÓNA A & GUREVICH B. 2016. Estimation of seismic attenuation and prediction of VTI anisotropy parameters from VSP and log data: a case study from the Middle East. Arabian Journal of Geosciences, 9(7): 485.

BACKUS G. 1962. Long-wave elastic anisotropy produced by horizontal layering. Journal of Geophysical Research, 67(11): 4427–4440.

BASSIOUNI Z. 1994. Theory, Measurement and Interpretation of Well Logs. Society of Petroleum Engineers, Richardson, Texas. 372 pp.

BOUCHAALA F, ALI M & MATSUSHIMA J. 2016. Attenuation modes from vertical seismic profiling and sonic waveform in a carbonate reservoir, Abu Dhabi, United Arab Emirates. Geophysical Prospecting, 64(4): 1030–1047.

FOX SMITH W. 2010. Waves and Oscillations. A Prelude to Quantum mechanics. Oxford University Press, New York. 432 pp.

KING G. 2009. Vibrations and waves. John Wiley & Sons, Ltd., West Sussex, England. 248 pp.

KJARTANSSON E. 1979. Constant Q-wave propagation and attenuation. Journal of Geophysical Research, 84(B9): 4737–4748.

LINER C. 2014. Long-wave elastic attenuation produced by horizontal layering. The Leading Edge, 33(6): 634–638.

PAIN H. 2005. The physics of vibrations and waves. 6th ed., John Wiley & Sons, Ltd., West Sussex, England. 556 pp.

PARRA J, ITURRARÁN-VIVEROS U, PARRA J & XU P. 2015. Attenuation and velocity estimation using rock physics and neural network methods for calibrating reflection seismograms. Interpretation, 3(1): 121–133.

QUAN Y & HARRIS J. 1997. Seismic attenuation tomography using the frequency shift method. Geophysics, 62(3): 895–905.

RUTLEDGE J & WINKLER H. 1989. Attenuation measurements from vertical seismic profile data: Leg 104, site 642. Proceedings of the Ocean Drilling Program, Scientific Results, 104: 965–972.

SHERIFF R & GELDART L. 1995. Exploration Seismology. 2nd ed., Cambridge University Press, New York. 628 pp.

SUZUKI H & MATSUSHIMA J. 2013. Quantifying uncertainties in attenuation estimation at methane-hydrate-bearing zones using sonic waveform logs. Geophysics, 75(5): 339–353.

TIWARY D, BAYUK I, VIKHOREV A & CHESNOKOV E. 2009. Comparison of seismic upscaling methods: From sonic to seismic. Geophysics, 74(2): 3–14.

Recebido em 20 abril, 2017 / Aceito em 19 fevereiro, 2018
Received on April 20, 2017 / Accepted on February 19, 2018